

## The Shape Of Optimal Magnetics: Why Flatter Is Better

by Dennis Feucht, Innovatia Laboratories, Cayo, Belize

What are the best designs for magnetic cores and windings that minimize their design constraints? The ultimate constraint on the design of transformers and coupled inductors (or *transductors*) is that the structure of the device not change after it is manufactured. Power loss in either the core or windings causes a rise in temperature that results in either a breakdown in winding insulation or a change in the core's magnetic structure. A design scheme that minimizes temperature rise prevents such damage to the windings or core, keeping the device within its safe operating limits.

This article examines design optimality from the standpoint of shape or geometry. By analyzing the impact of device geometries on core and winding temperatures, some insights are gained into the optimal shapes for cores, conductors and winding configurations. This analysis ultimately recommends the use of flatter structures to the extent allowed by other design constraints.

### Optimal Core Shape

Minimization of core power loss is a design goal, but a more basic goal is to constrain maximum core temperature. If core thermal resistance,  $\theta_c$ , is minimized, then core power loss,  $P_c$ , can be increased subject to the maximum allowed temperature rise,  $\Delta T$ :

$$\bar{P}_c = \bar{p}_c \cdot V = \frac{\Delta T}{R_\theta} = G_\theta \cdot \Delta T \Rightarrow \bar{p}_c = \frac{G_\theta}{V} \cdot \Delta T = (\sigma_\theta \cdot \Delta T) \cdot \left( \frac{A_s}{l \cdot V} \right)$$

where  $\bar{p}_c$  represents average core power-loss density,  $V$  is volume,  $R_\theta$  is thermal resistance,  $G_\theta$  is thermal conductance,  $\sigma_\theta$  is thermal conductivity,  $A_s$  is surface area, and  $l$  is thermal path length. The terms  $\bar{p}_c$  and  $\sigma_\theta$ , are fixed by the given core material thermal property and  $\Delta T$  is fixed by design. Thus  $\sigma_\theta \cdot \Delta T$  is a constant and  $A_s$ ,  $V$ , and  $l$  are size-dependent.

The performance parameter to be maximized for minimum temperature is the geometric ratio,  $A_s/l \cdot V$ . For a relatively uniform field distribution in the core, its power dissipation is uniform throughout the core volume,  $V$ , and scales with  $V$ . The resulting heat travels a characteristic path length of  $l$ , then leaves the core via the thermal path that crosses the core surface. Analogous to electrical conduction, surface area is the cross-sectional area of the thermal path. As it is increased, heat has a greater area through which to leave the core and thermal resistance is decreased.

$A_s$  and  $V$  can be derived geometrically from core dimensions. For complicated shapes,  $l$  can be difficult to determine accurately but varies as  $V^{1/3}$ ; it scales with volume.  $A_s/l \cdot V$  of a sphere, where  $l = r$ , is

$$\frac{A_s}{l \cdot V} (\text{sphere}) = \frac{4 \cdot \pi \cdot r^2}{r \cdot \left( \frac{4}{3} \cdot \pi \cdot r^3 \right)} = \frac{3}{r^2} = \text{constant} \cdot \frac{1}{V^{2/3}}$$

Different core shapes of equal volumes will have differing  $A_s$  but  $A_s/l \cdot V$  for all cores scales by  $1/(\text{length})^2$  or  $1/V^{2/3}$ . Thus a size-independent thermal comparison of shapes can be based on  $A_s/V^{2/3}$ . For a sphere, which is the worst-case shape,

$$\frac{A_s}{V^{2/3}} (\text{sphere}) = (36 \cdot \pi)^{1/3} \approx 4.836$$

The ratio of  $A_s/V^{2/3}$  for a shape normalized to that of a sphere is the *thermal shape factor*, defined as

$$\Xi_{\theta} \equiv \frac{\left. \frac{A_s}{V^{2/3}} \right|_{\text{shape}}}{\left. \frac{A_s}{V^{2/3}} \right|_{\text{sphere}}} = \frac{\left. \frac{A_s}{V^{2/3}} \right|_{\text{shape}}}{(36 \cdot \pi)^{1/3}} \approx \frac{\left. \frac{A_s}{V^{2/3}} \right|_{\text{shape}}}{4.836} \geq 1.$$

$\Xi_{\theta}$  varies with core shape but not size. For complicated shapes with multiple dimensions, the above formula gives  $\Xi_{\theta}$  for a given core from  $A_s$  and  $V$ . Then  $\bar{p}_c$  is calculated from  $\bar{p}_c(\text{sphere})$  and  $\Xi_{\theta}$ :

$$\bar{p}_c = \Xi_{\theta} \cdot \bar{p}_c(\text{sphere}).$$

As an example shape, consider the simple cube. A cube of side length  $s$  has

$$\frac{A_s}{V^{2/3}} = \frac{6 \cdot s^2}{(s^3)^{2/3}} = 6.$$

Then the thermal shape factor is

$$\Xi_{\theta}(\text{cube}) \approx \frac{A_s / V^{2/3}}{4.836} = \frac{6}{4.836} \approx 1.241.$$

The cube surface area is greater than that of a sphere of the same volume by about 24%.

For a cube circumscribed on a sphere, equate volumes, and the length,  $s$ , of a side of the cube is solved in  $r$  of the sphere:

$$s^3 = \frac{4}{3} \cdot \pi \cdot r^3 \Rightarrow s = \sqrt[3]{\frac{4}{3} \cdot \pi} \cdot r \approx 1.612 \cdot r.$$

The cube has  $s = 2 \cdot r$ , and for this larger size of cube,

$$\frac{A_s}{l \cdot V} = \frac{6 \cdot (2 \cdot r)^2}{r \cdot (2 \cdot r)^3} = \frac{3}{r^2}$$

which is the same as for the sphere. However, because  $A_s/l \cdot V$  scales with size ( $V$  or  $r$ ), the comparison is not valid; the sphere has nearly half the volume of the cube (by  $\pi/6 \approx 0.524$ ) and this reduces its ratio.

A toroid of rectangular cross-section with outer and inner radii of  $r_o$  and  $r_i$ , has an average radius,

$$\bar{r} = \frac{r_o + r_i}{2} = \frac{OD + ID}{4}$$

and height of  $h$ , with width

$$w = \Delta r = r_o - r_i = \frac{OD - ID}{2} = 2 \cdot (r_o - \bar{r}) = 2 \cdot (\bar{r} - r_i).$$

Then the toroid volume is

$$V = h \cdot \pi \cdot (r_o^2 - r_i^2)$$

and is the difference in volume of two disks. After some algebra, the ratio

$$\frac{A_s}{V^{2/3}} = 2 \cdot (2 \cdot \pi)^{1/3} \cdot \left( \left[ \left( \frac{h}{w^2} \right)^{1/3} + \left( \frac{w}{h^2} \right)^{1/3} \right] \cdot \bar{r}^{1/3} \right).$$

The constant,  $2 \cdot (2 \cdot \pi)^{1/3} \approx 3.691$ . Then for a rectangular toroid, the constant within  $\Xi_\theta$  is  $3.691/4.836 \approx 0.7631$ ;

$$\Xi_\theta(\text{rect toroid}) \approx 0.7631 \cdot \left[ \left( \frac{h}{w^2} \right)^{1/3} + \left( \frac{w}{h^2} \right)^{1/3} \right] \cdot \bar{r}^{1/3}.$$

For a square toroid,  $w = h$ , and

$$\frac{A_s}{V^{2/3}} = \frac{(4 \cdot h) \cdot (2 \cdot \pi \cdot \bar{r})}{[h^2 \cdot (2 \cdot \pi \cdot \bar{r})]^{2/3}} = (4 \cdot \sqrt[3]{2 \cdot \pi}) \cdot \left( \frac{\bar{r}}{h} \right)^{1/3} \approx (7.381) \cdot \left( \frac{\bar{r}}{h} \right)^{1/3}.$$

Then

$$\Xi_\theta(\text{square toroid}) \approx \frac{7.381}{4.836} \cdot \left( \frac{\bar{r}}{h} \right)^{1/3} = (1.526) \cdot \left( \frac{\bar{r}}{h} \right)^{1/3}.$$

For a square toroid,  $h \geq 2 \cdot \bar{r}$ , and the worst-case is one with no window, for which  $h = 2 \cdot \bar{r}$ . Then  $\Xi_\theta \approx (1.526) \cdot (0.5)^{1/3} \approx 1.22$ . This degenerate toroid is a disk with radius  $\bar{r}$  and thickness or height,  $h$ .

For a more realistic toroid having the same volume as a sphere of radius  $r = \bar{r}$ , then equating volumes of sphere and square toroid and solving,  $\Xi_\theta \approx 1.63$ . A square toroid allows 63% more  $\bar{p}_c$  than for a sphere with radius  $r = \bar{r}$ .

Some Micrometals rectangular toroids (with slightly rounded vertices) are given in Table 1 with calculated thermal quantities.

Table 1. Thermal shape factor ( $\Xi_{\theta}$ ) for various rectangular toroids.

Core	$\bar{r}$ (mm)	(mm)	$h$ (mm)	$V$ (mm <sup>3</sup> )	$A_s$ (mm <sup>2</sup> )	$\Xi_{\theta}$
T26	1.83	2.03	4.83	113	158	1.40
T50	5.10	2.50	4.83	387	470	1.83
T50D	5.10	2.50	9.53	763.5	771	1.91
T80	8.20	3.80	9.53	1866	1374	1.88
T130	13.2	6.60	11.1	6076	2936	1.82
T131	12.325	8.35	11.1	7180	3012	1.67
T250	23.83	15.85	25.4	60280	12350	1.66

The core catalog magnetic volumes are 5% to 10% smaller than the geometrically-calculated volumes from nominal lengths in Table 1. Some variation in  $\Xi_{\theta}$  occurs among the core sizes with an average of 1.74. If all but the smallest are averaged, the result is

$$\Xi_{\theta}(\text{rectangular toroid}) \approx 1.8$$

with a deviation of 0.11. The improvement of about 10% over  $\Xi_{\theta}$  (square toroid)  $\approx 1.63$  is expected in that the square cross-section is the worst rectangular shape. Toroids are the most thermally efficient of the standard core shapes and can dissipate about 80% more power than a sphere for the same  $\Delta T$ .

$A_s/V$  varies with dimensional reduction by  $n/r$  where  $n$  is the dimensionality of the core shape—for the sphere, by  $3/r$ , and toroids by  $2/r$ , whether circular or rectangular in cross-section. A prism with an arbitrary planar shape of area  $A_p$  and thickness dimension,  $h$ , decreasing so that in the limit  $h$  approaches zero, the shape approximates a magnetic film, and

$$\frac{A_s}{V} = \lim_{h \rightarrow 0} \frac{A_s(h)}{h \cdot A_p} \approx \lim_{h \rightarrow 0} \frac{2 \cdot A_p}{h \cdot A_p} = \lim_{h \rightarrow 0} \frac{2}{h} \rightarrow \infty .$$

The closest core shape to that of a film—an approximately 2D shape—is the *planar* core. If the shape in 2D has greatly-differing dimensions, it approaches a line in shape like toroids for which  $\bar{r} \gg w$ . A 1D shape has even better thermal performance.

Calculations for various core shapes result in Table 2. For a given core shape, it gives the multiplier of how much more power the shape can dissipate than that of a sphere of equal volume.

Table 2. Thermal shape factor ( $\bar{\epsilon}_\theta$ ) for various core shapes.

Core Shape, 2 cm <sup>3</sup>	$\bar{\epsilon}_\theta = \frac{\bar{p}_c}{\bar{p}_c(\text{sphere})}$
square toroid	1.63
round toroid	1.47
EE	1.55
ETD	1.8
pot	1.09 (1.72)

Design tables of core characteristics can include the allowable  $\bar{p}_c$  for particular cores of a given shape by calculating  $\bar{p}_c(\text{sphere})$  for the volume of the core and using the thermal shape-factor table above to list  $\bar{p}_c$ . The formula for  $\bar{p}_c(\text{sphere})$  was derived in a previous article, "[How to Choose Magnetic Core Size](#)" (*How2Power Today*, May 2013 issue.)

### Optimal Wire And Winding Shapes

Electrical loss in wire results from static resistance. More significantly in switching converter transducers, it is a result of dynamic or frequency-dependent losses caused by the skin and proximity effects. They are essentially the same effect; the skin effect produces loss in a given wire while the proximity effect produces loss in the wires in proximity to a given wire. The ratio of dynamic to static resistance is an indicator of the extent of the dynamic loss:

$$F_R = \frac{R(f)}{R_0}$$

where  $R(f)$  is the frequency-dependent (skin-effect) resistance and  $R_0$  is the static (0 Hz) resistance.

A parameter used to characterize dynamic resistance is the *skin depth*,  $\delta$ . Ideally,  $\delta = 0$  and there is no dynamic winding loss. The *skin-depth ratio* is the ratio of wire radius to skin depth, where  $r_c$  is the wire conductive radius;

$$\xi = \frac{r_c}{\delta}$$

Here  $\xi$  indicates how much the skin effect increases  $F_R$  and applies to a winding of a given wire size. Ideally,  $\xi = 0$  and the skin depth is infinite—the case for static current for which  $F_R = 1$ . To achieve this ideal,  $\delta$  is determined for a given conductor material (Cu or Al) and switching frequency. Thus  $r_c$  is made as small as possible to minimize  $\xi$ . Either a bundle of small (low  $r_c$ ) wires or foil is used.

Foil thickness relates simply to  $r_c$ . Just as a planar core is optimal for the magnetic side of the transducer design, planar windings are optimal for the electrical side. Very thin conductors approach the shape of conductive film and are either foil or circuit-board traces. Foil is geometrically more compatible with winding windows of non-planar cores, and etched circuit-boards (ECBs), stamped metal turns, or metalized polyimide film are preferred methods for winding construction for low-height windings. ECB fabrication technology is geometrically precise and results in a low tolerance of parasitic reactance in transducers, especially if layers of

thin ECB material can be stacked using an accurate alignment method such as notches or pilot holes through the boards.

Planar magnetics and planar windings are combined in a newer kind of transductor construction as shown in the figure below with stamped-metal turns.

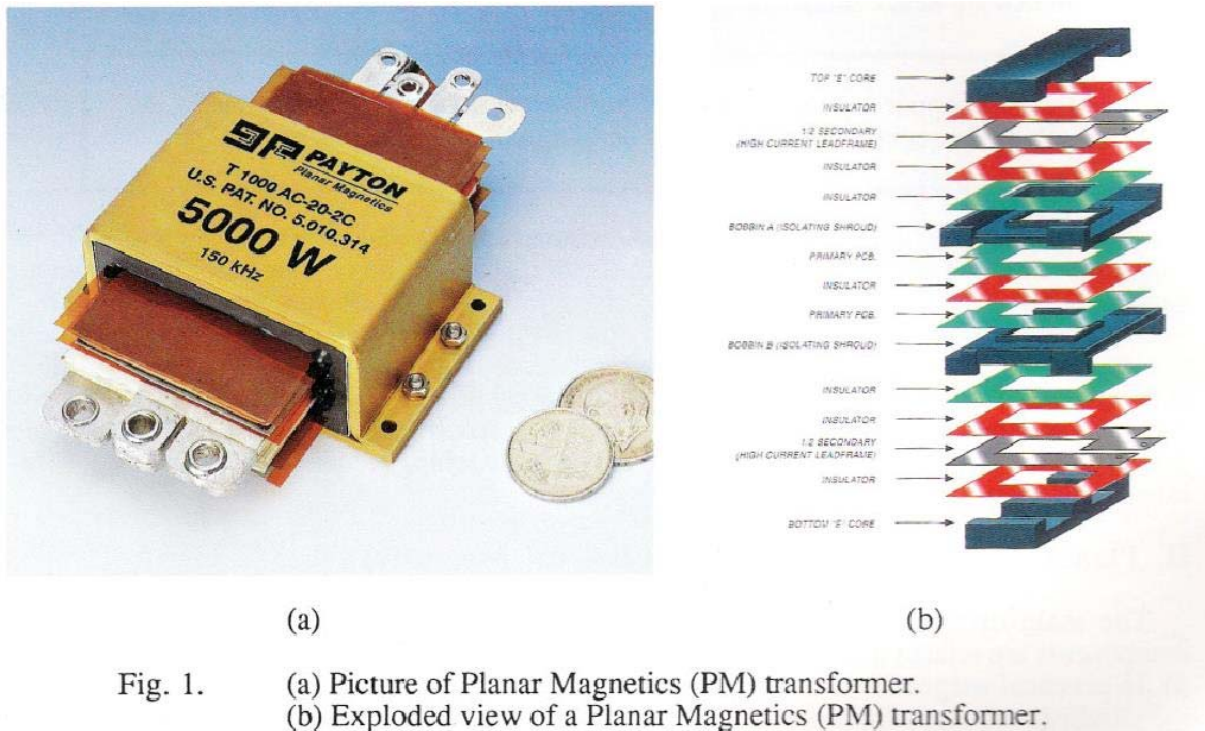


Fig. 1. (a) Picture of Planar Magnetics (PM) transformer.  
 (b) Exploded view of a Planar Magnetics (PM) transformer.

Figure. Planar magnetics transformer and a cross section showing its construction. [Source: "The Benefits of Planar Magnetics in HF Power Conversion," Prof. Sam Ben-Yaakov, Ben-Gurion U. of the Negev, Israel, page 2, from Payton Planar Magnetics Catalogs: DC/DC, AC/DC, 1994.]

One of the apparent limitations of ECB windings is that they are turns-limited—or so it might seem. ECB technology, like that of monolithic integrated circuits, has steadily shrunk its working dimensions so that for more than a decade, 25- $\mu\text{m}$  (1-mil) traces with 25- $\mu\text{m}$  spacing have been available in production. Such traces are equivalent to double-insulated (heavy) #38-AWG wire, good for about 37 mA. On a single side of a board, 100 turns has a winding width of 5 mm.

A significant disadvantage of ECB windings over magnet wire is the *packing factor*,  $k_p$ . For equal trace width and spacing, half the area is lost to nonconductor and  $k_p \leq 1/2$ . If the ECBs used are kapton or other 50- $\mu\text{m}$  film, then each trace is surrounded by 50- $\mu\text{m}$  non-conductive space, and for trace width and height  $w$ ,

$$k_p = \frac{w^2}{(2 \cdot w)^2} = \frac{1}{4}$$

This  $k_p$  is comparable to that of a #37-AWG magnet wire. Its multilayer  $k_p \approx 1/2.52$ , better than the film-ECB winding.

An additional comparison with magnet-wire windings is that the insulation breakdown voltage of a heavy wire is about 700 V whereas the comparable breakdown spacing between adjacent ECB traces is over 5 mm. Spacing can be reduced with board coatings such as solder mask. With windings on opposite sides of the board, ECBs are comparable or higher in breakdown voltage to enamel on magnet wires.

Finally, the winding configuration has a shape. The two main categories are *concentric* windings, applied serially to the bobbin window, or *multifilar* windings, wound in parallel instead.

The multifilar option places all the wires of all windings in close proximity so that the differential voltages across them along their lengths are zero, and their winding areas are closely matched. This results in low parasitic capacitive currents and low leakage inductances. Thin ECBs having the same trace patterns are the counterpart to magnet-wire multifilar bundles.

For either winding scheme, additional winding layers quickly increase  $F_R$  and electrical loss. One layer is optimal for the winding. As with magnetic cores, the optimal shape is 2D, both for the conductor itself and the winding configuration. The shape of conductor that approaches 2D is a *circuit-board trace*, a stamped turn, or a *foil*. The shape of winding is single-layer, bundled to minimize  $F_R$ .

Transducers and their components have optimal 2D shapes, though these shapes cannot always be achieved in practice because of other design criteria. Here, some of the most important have been considered, and they can guide design by informing our visual memory of what to look for that is best in a transducer shape: reduced dimensionality.

### **About The Author**



*Dennis Feucht has been involved in power electronics for 25 years, designing motor-drives and power converters. He has an instrument background from Tektronix, where he designed test and measurement equipment and did research in Tek Labs. He has lately been doing current-loop converter modeling and converter optimization.*

For more on magnetics design, see the How2Power Design Guide, select the [Advanced Search](#) option, go to Search by Design Guide Category, and select "Magnetics" in the Design Area category.